Computational and experimental investigation of mixing in microchannels

Katia LAGANÀ[1,*], Margherita CIOFFI[1,2], Francesca NASON[1], Elena ROMANELLI[1], Giancarlo PENNATI[1], Gabriele DUBINI[1]

* Corresponding author: Tel.: ++39 02 23994293; Fax: ++39 02 23994286; Email: katia.lagana@polimi.it
1: Laboratory of Biological Structure Mechanics, Department of Structural Engineering, Politecnico di Milano, Milan, Italy
2: IRCCS Istituto Ortopedico Galeazzi, Milan, Italy

Abstract Mixing is a key process for the successful of all chemical or biochemical reactions, so effective micromixers represent essential components for micro total analysis systems (µTAS) or lab-on-a-chip. In the present study a combined computational and experimental approach was adopted to evaluate how the efficiency of a Y-mixer can be enhanced by modifying its downstream geometry. Three different geometries were studied and compared: Y-straight channel, Y-sine channel and Y-wrinkled wall channel. For each of them the influence of perfusing flow rates and channel cross section aspect ratio was investigated. Physical prototypes were built using a simple technique based on a xerographic process, and their mixing performance was experimentally evaluated. Computational models of the designed micromixers were generated: the Navier-Stokes equations for an incompressible Newtonian fluid and the advection-diffusion equation were solved with an uncoupled approach by means of the finite volume method. The computational and experimental results were critically compared, revealing Y-wrinkled wall mixer as the best performer among those considered and suggesting criteria of possible improvements and optimization.

**Keywords:** Micromixer, CFD, Experimental measurement, Flow mixing

1. Introduction

The recent trend in analytical chemistry and life science is miniaturization of fluid handling and analysis, which emerges in the field of microfluidics. Microfluidic applications cover micro arrays, sample preparation and analysis, cell separation and detection, and environmental monitoring (Nguyen and Wu, 2005). Most microfluidic systems operate in a laminar flow regime dominated by molecular diffusion, which is not favourable to mixing (Graveson et al., 1993). Mixing is a key process for the successful of all chemical or biochemical reactions. The absence of turbulence, the primary mechanism for macroscale mixing, have spurred to investigate alternative strategies for mixing in microfluidic systems. Hence, effective micromixers represent essential components for micro total analysis systems (µTAS) or lab-on-a-chip. In general micromixers can be classified as active or passive. The former use an external source to generate a disturbance on the fluid field to enhance the mixing process, while the latter rely entirely on diffusion or chaotic advection, and achieve mixing using only the geometry of the channel (Nguyen and Wu, 2005). In particular, passive micromixers aim to increase the interface between the different fluids so as to improve molecular diffusion and reduce the mixing path. Examples of such micromixers are serial or parallel laminating-, split and recombine-, chaotic-, recirculation flow-mixers (Hessel et al., 2005).

In the present study a combined computational and experimental approach was adopted to evaluate how the efficiency of a Y-mixer can be enhanced by modifying its downstream geometry. Three different geometries were considered, and the influence of perfusion flow rates and channel cross section shape (aspect ratio) was investigated for each of them. The experimental and computational results were critically compared, and useful design indications to improve mixing efficiency were extracted.

2. Material and methods

Three different geometries were studied and compared: Y-straight channel, Y-sine channel and Y-wrinkled wall channel as indicated in Fig.1 (a-c). Three different channel widths were analyzed (150-180-200 μm) for each geometry.
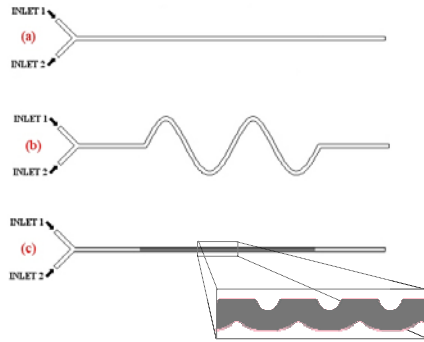
Fig. 1. Layouts of the micromixers: (a) Y-straight channel; (b) Y-sine channel; (c) Y-wrinkled wall channel.

2.1 Fabrication of the micromixers

A simple, low-cost and rapid one-step method for design and fabrication of passive micromixers based on a xerographic process was adopted (do Lago et al., 2003; Liu et al., 2005). Figure 2 shows the complete process to obtain the devices.
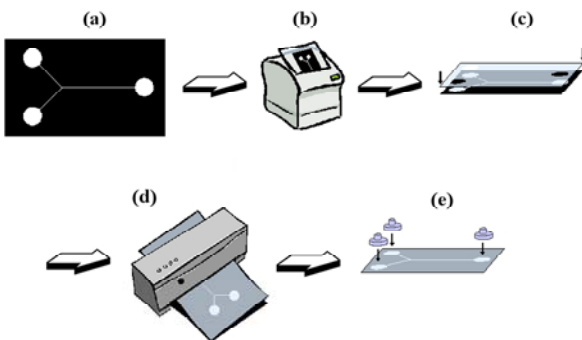

Fig. 2 – Schematic of the fabrication process: (a) layout design; (b) laser-printing process; (c) superimposition of the two transparencies; (d) lamination process; (e) gluing of reservoirs.

A laser printer (LaserJet Epson ELP6100, set to 1200dpi) was used to selectively deposit toner on a transparency film CG3300 (3M Italy S.p.A.). It was subsequently laminated against another transparency film (Laminator 330, GBC) at 130 °C, repeating the process for three times. The toner layer binds the two transparencies and allows the blank regions to become channels for microfluidics. Reservoirs were glued at the channels extremities where holes were previously drilled on the white film. The depth of the so-fabricated microchannel is determined by the thickness of the ink deposited on the transparency film. For Y-wrinkled wall channel wrinkles were obtained with a grey level of 30%.

2.2 Experimental characterization of the devices

The toner layer thickness was measured before lamination using a laser profilometer (UBM Microfocus). An average value of 8 μm was found (Fig. 3).
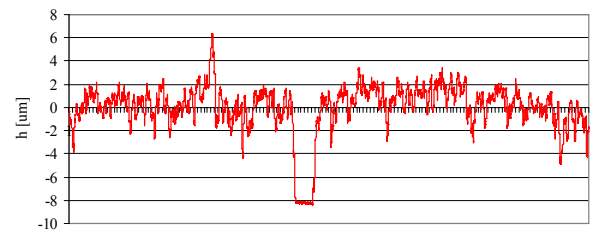
Fig. 3. Example of pattern generated by a profilometer for a 200 μm-wide microchannel.

The printer resolution and the toner particle size affect the quality of the produced channel. Indeed, as shown in Fig. 4 (top), the channel definition is quite poor due to irregular toner deposition at the borders.
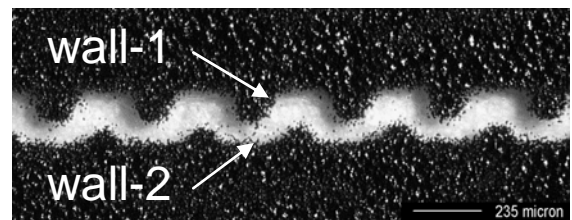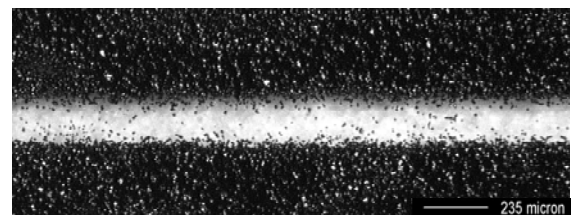

Fig.4. Light microscope image of the Y-straight 150 μm-wide channel (top) and the Y-wrinkled wall 200 μm-wide channel (bottom).

The micromixer obtained setting the printing at 30% grey level in the microchannel is shown in Fig. 4 (bottom): the walls resulted wrinkled with different geometries on the opposite walls (indicated in the following as wall-1 and wall-2). The channel width was checked after the lamination process and measures performed on light microscope images revealed a constant reduction of 15 μm, while the channel depth was unchanged.

2.3 Mixing experiments

A tracer dye was used to quantify the extent of mixing. The two inlets of the microdevices were perfused by means of a two- parallel-channel syringe pump (Harvard 712001, 1 ml syringes), one filled with deionised water and the other with a red food dye. The mixing was observed under optical microscope for three different flow rates (0.06-0.36-0.72 μl/min) and images were recorded after reaching steady stationary conditions (Fig.5).
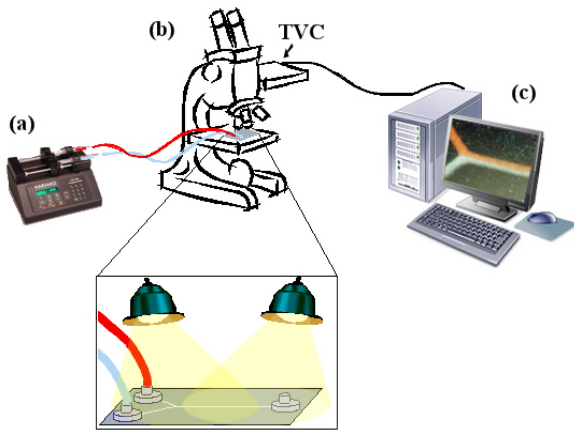

Fig. 5. Experimental set-up: (a) syringe pump; (b) microscope; (c) PC

Colour intensity in the micro-channel image is proportional to dye concentration (Fig.6). Each coloured image was converted into a grey scale one. Pixel grey level was determined for channel cross sections at different distance from the inlet. The concentration trend across the channel indicates the achieved mixing. According to Sudarsan and Ugaz (2006) the mixing efficiency was quantified by computing the standard deviation of the intensity distribution over several cross-channel lines at different distance from the inlets:

$$IM_C = \sqrt{\frac{n \cdot \sum C^2 - \left(\sum C\right)^2}{n \cdot (n-1)}} \qquad (1)$$

where IM is the index of mixing, C is the grayscale value of each pixel (scaled between 0 and 1) and n is the number of pixel of each cross section line. Thus IM=0.5 corresponds to completely unmixed regions whereas IM=0 corresponds to complete mixing.
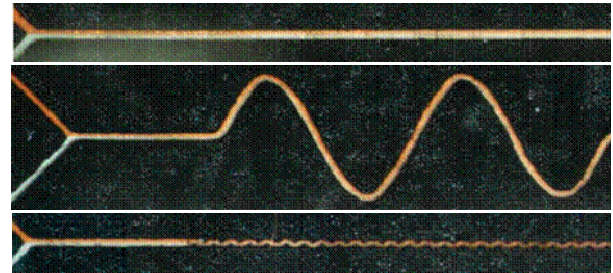
Fig. 6. Recorded images of the experimental tests for the Y-straight (top), Y-sine (middle) and Y-wrinkled wall mixers

2.4 Computational models

CAD models of each geometry and their meshes were generated by means of the solid modeler GAMBIT (Ansys Inc., Canonsburg, PA, USA). Steady state simulations were carried out using the finite volume code FLUENT (Ansys Inc., Canonsburg, PA, USA). The steady-state Navier-Stokes equations for an incompressible Newtonian fluid were solved:

$$\begin{cases} \rho(\vec{v} \cdot \nabla)\vec{v} = -\nabla p + \mu \nabla^2 \vec{v} \\ \nabla \cdot \vec{v} = 0 \end{cases} \qquad (2)$$

where $\vec{v}$ and p are the velocity vector and pressure respectively. The density ρ and the viscosity μ were measured for both deionised water and dye and quite similar values were found (ρ=1000 kg/m^3 and μ =1.04·10^{-3} Pa·s). Hence, the advection-diffusion equation was subsequentially solved with an uncoupled approach:

$$\frac{\partial \rho c}{\partial t} + \rho \vec{v} \cdot \nabla c = \nabla \cdot (D\nabla c) \qquad (3)$$

where c is the concentration of the diffusing species. Dye diffusivity in water was experimentally measured and set to $1.5 \cdot 10^{-9} m^2/s$, in agreement with values suggested by Nguyen and Wu (2005). Equal flow rates with flat velocity profiles were applied at the two inlets. Three different flow rates were investigated according to the experimental tests. Zero pressure was imposed at the outlet. No-slip conditions were applied to the walls. Uniform dye concentrations (0 and 1) were imposed on the two inlets. Zero diffusive flux was applied at the outlet.

As done for the experimental results, mixing efficiency was evaluated by means of IM_c, according to equation (1), where C now is the concentration corresponding to a single mesh volume.

For the flow rates and the channel dimensions adopted, Reynolds number (Re) are too low ($10^{-3} \div 10^{-2}$) to generate significant advection phenomena, which require $10 < Re < 100$ (Nguyen and Wu, 2005). Since advection play an important role in increasing mixing efficiency, a few additional computational simulations were carried out for the Y-sine and Y-wrinkled wall 185 μm-wide channels increasing flow rate and height of the channel (up to 185 μm) to increase Re. The beneficial effect on mixing was evaluated on the basis of the percentage "folding" of the interface between the two color fluids.

Finally, different layouts of wrinkles for the Y-wrinkled wall channel were investigated in order to evaluate the influence of the corrugated profiles on the flow path and therefore on the mixing. Three different channel models were implemented: i) asymmetric walls as that obtained in the built microdevices, ii) and iii) symmetric walls according to the wall-1 and wall-2 geometries (Fig.4-bottom).

3. Results and discussion

Figures 7-8 show the trends of IM_c along the Y-straight channel at three different flow rates and for three different channel widths, respectively. The graphs show the

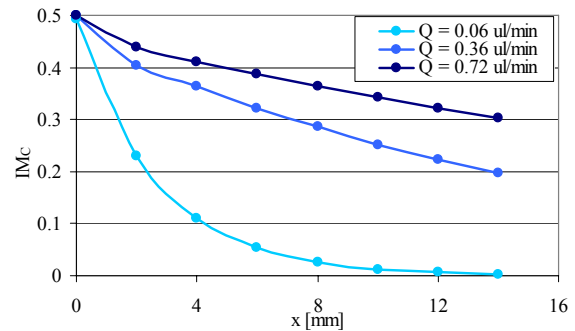computational results but similar behaviours were obtained in the experimental tests.

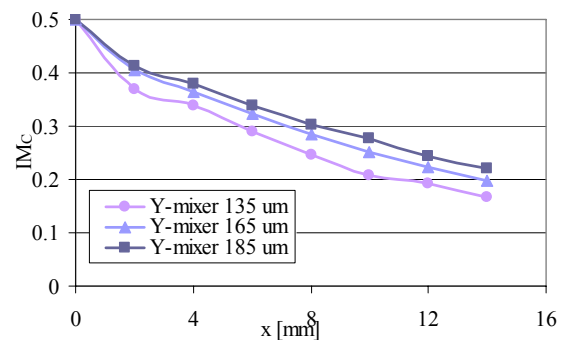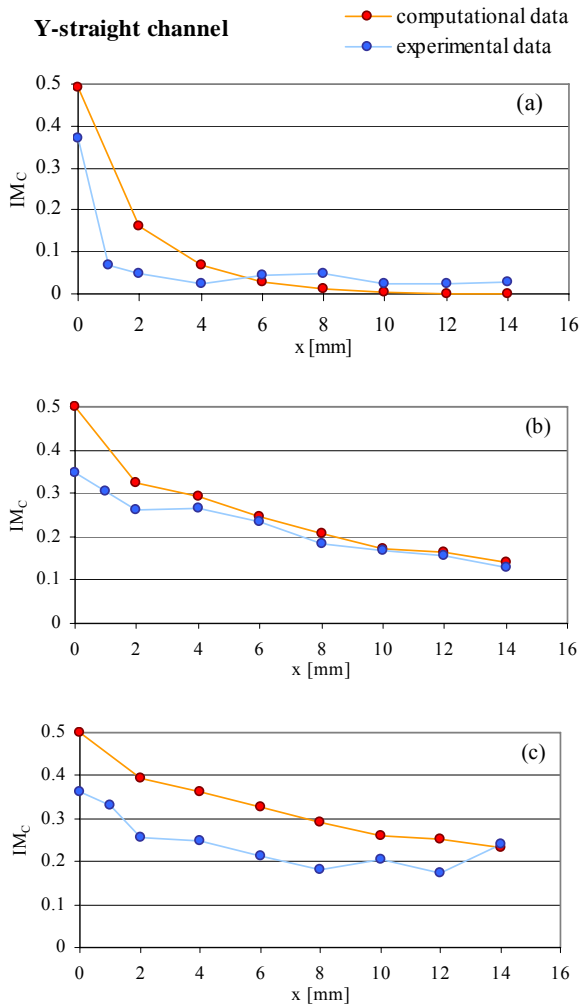**Fig. 7.** IM_c trends for Y-straight 165-μm-wide channel for three different flow rates.

Fig. 8. IM_c trends for Y-straight channels of three different widths, perfused at 0.36 μl/min.

As expected, in the straight channel the mixing decreases at increasing flow rates, indeed when only diffusion occurs the length of mixing is proportional to the fluid velocity at constant diffusion time (Cussler, 1996). Instead, a larger channel (with fixed depth and flow rate) is characterized by a higher diffusion time, so that a longer channel is necessary to reach mixing for the same flow rate (Cussler, 1996).

A comparison between the computational and experimental results obtained for the Y-straight channel is shown in Fig.9. The graphs show quite a good agreement between experimental and computational trends, but the difference between the data at the inlet of the mixing channel is not negligible. Nevertheless, the concentration profile at the inlet of mixing channel does not depend on model reliability since it is directly connected to the imposed boundary conditions. The computational simulations highlight a value of IM=0.5, in agreement with a complete separation between

the two fluids, while the experiments showed a lower value of 0.35, clearly due to experimental measurement errors. With the adopted experimental set-up (lights, camera resolution, focusing system) the recorded images were not sharp enough to reveal the perfect separation actually occurring between the two fluids: hence, the experimental data always overestimated the mixing at the inlet of the channel.


Fig. 9. Comparison between the experimental and computational IM trends for Y-straight 135-μm-wide channel for flow rates of: (a) 0.06 μl/min; (b) 0.36 μl/min; (c) 0.72 μl/min.

The data obtained for the Y-sine mixer are not graphically reported, but it was observed that its performance are the same as the Y-straight mixer if the actual length covered by the fluids is considered. Hence, for the 8μm depth channels convective phenomena are not involved and the Y-sine channel, with wavy

shape, just allows to reduce the device axial dimension (-17 %) necessary for a complete mixing.

Conversely, the Y-wrinkled wall channels showed to enhance mixing. To compare the performance of the three studied geometries, Y-straight, Y-sine and Y-wrinkled wall channels, the length of the device necessary to reach a fixed partial mixing ($IM_c = 0.3$, i.e. mixing of 40%) was graphed vs. the perfusing flow rates (Fig.10).
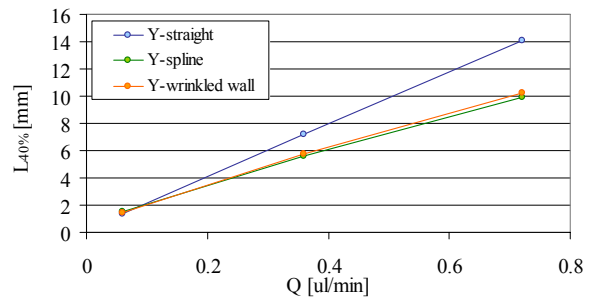

Fig. 10. Distance from the inlet necessary to reach the mixing of 40% at different flow rates in Y-straight, Y-sine and Y-wrinkled wall 165-μm-wide channels.

The graph highlights how much beneficial can be a geometrical modification of the microchannels on the mixing phenomena. The Y-wrinkled wall micromixer seems to improve mixing as well as the Y-sine micromixer. They are comparable if the device axial dimension is considered, but since the distance covered by the fluids is different for the two mixers, the time of mixing is reduced for Y-wrinkled wall one, making it the best performer.

The simulation results for the Y-sine and Y-wrinkled wall channels with increased depth are shown in Figs.11-12.
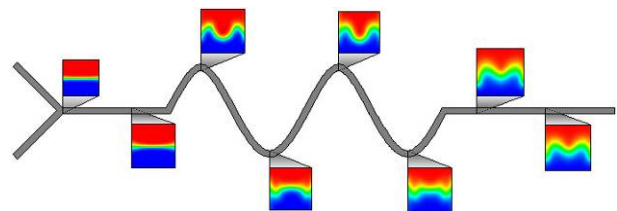

Fig. 11. Cross-sectional concentration profiles along the Y-sine 185 μm × 185 μm mixing channel at v = 11cm/s
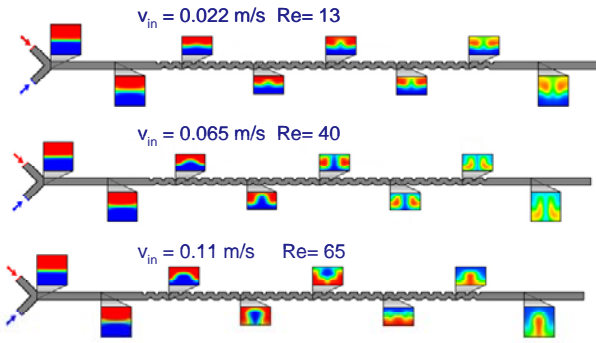
Fig. 12. Cross-sectional concentration profiles along the Y-wrinkled wall 185 μm × 185 μm mixing channel at different flow rates.

When the microchannel are deeper and the velocity higher (i.e. higher Re), secondary motions are generated. These secondary motions result in folding the interface between the two fluids, leading to an enhanced diffusion and so improving mixing. However, these secondary motions can provoke the twisting of the two fluids, causing an inverted concentration profile at the outlet compared to the inlet (Re equal 40 and 65) . The increase of the interface was quantified and is shown in Figs.13-14, for the Y-sine and Y-wrinkled wall mixers, respectively.
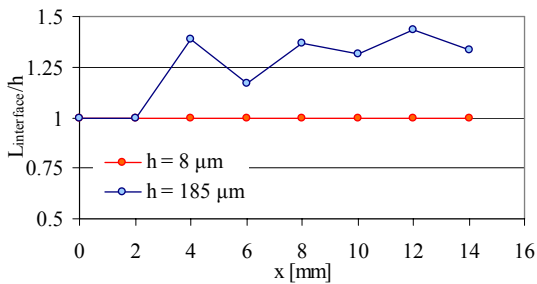

Fig. 13. Increase per unit of depth of the interface between the fluids for Y-sine 185 μm-wide channel.
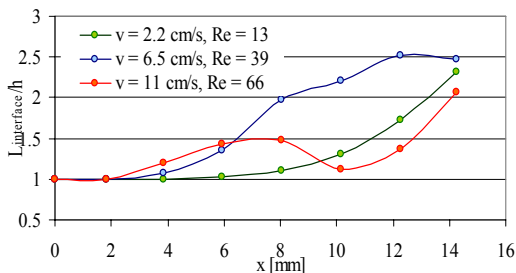
Fig. 14. Increase per unit of depth of the interface between the fluids for Y-wrinkled wall 185 μm × 185 μm mixing channel.

From Fig. 14 it can be noticed that for the Y-wrinkled wall channel the best mixing performance is obtained with an intermediate velocity, which means that an optimization process would be necessary.
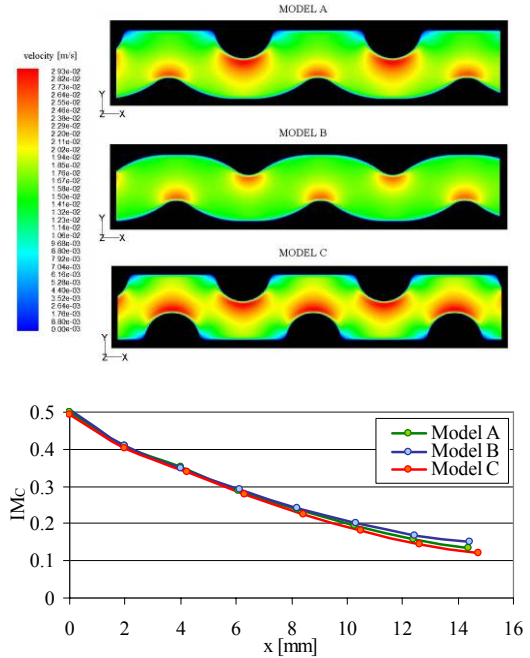
Fig. 15. Contour of velocity magnitude for the three wrinkle layouts considered (top); IM_c trends for the three models (bottom).

Moreover, the study of different wrinkle layouts, for very low channel depth (8 μm) and Re revealed their influence on the mixing phenomenon as shown in Fig.15.

3. Conclusions

For the 8μm-deep micromixer at low Re a good agreement between the experimental and the computational results was found, suggesting the Y-wrinkled mixer as the best performer. Moreover the additional computational analysis carried out on the wall morphology of the Y-wrinkled mixer showed how local geometrical details can improve mixing. The simulation performed on square cross-section micromixers at high Re, revealed the complexity of the phenomena involved in the mixing (flow twisting, interface folding) when secondary motion are generated, suggesting the computational approach as essential for design optimization.

References

Cussler, E.L., 1996. Diffusion mass transfer in fluid systems. 2nd ed., New York: Cambridge University Press.

do Lago, C.L., da Silva, H.D., Neves, C.A., Brito-Neto, J.G., da Silva, J.A., 2003. A dry process for production of microfluidic devices based on lamination of laser-printed polyester films. Anal. Chem. 75(15), 3853-8.

Graveson, P., Branjeberg, J., Jensen, O.S., 1993. Microfluidics-a review. J Micromech Microeng. 3(4), 168-182.

Hessel, V., Lowe, H., Schonfeld, F., 2005. Micromixers-a review on passive and active mixing principles. Chem Eng Sci. 60, 2479-2501.

Liu, A.L., He, F.Y., Wang, K., Zhou, T., Lu, Y., Xia, X.H., 2005. Rapid method for design and fabbrication of passive micromixers in microfluidic devices using a direct-printing process. Lab Chip. 5(9), 974-978.

Nguyen, N.T. and Wu, Z., 2005. Micromixers- a review. J Micromech Microeng. 15, R1-R16.

Sudarsan A.P., Ugaz V.M., 2006. Multivortex micromixing. PNAS 103(19), 7228-7233.